Residue analysis in linearized elastic inversion

PP4.13

Aart-Jan van Wijngaarden and Cornelis P.A. Wapenaar; Delft University of Technology*

Summary

Amplitude-versus-Offset (AVA)information is used for estimation of the elastic parameters. We introduce a method based on the linearized Zoeppritz equation to separate the linear AVA behavior from the nonlinear and noise terms, which we call the residue. This residue is used to analyze the influence of errors, noise and nonlinear terms on the resolution of the linear inversion. The problem of interference of thin layers has been addressed and a new method to avoid the apparent AVA due to this layering is shown.

Introduction

An important property in the detection of hydrocarbon deposits is the way seismic waves vary in amplitude as a function of incidence angle, when being reflected from a buried rock interface. Careful measurements of these small amplitude varations may be combined in an inversion scheme to estimate the elastic parameters. The inversion of Amplitude-versus-offset (AVO) or Amplitude-versus-Angle (AVA)s generally based on Zoeppritz for isolated reflectors. For small angels of incidence and small contrasts in the elastic parameters these equations can be linearized [Aki and Richards, 1980]. The outcome of the inversion depends on the quality of the input data, on the parametrization of the theoretical model and on the violations of the assumptions in the theoretical model. In this paper we analyze the influence of these three factors on the residue of the inversion process.

Constrained linearized elastic inversion

The linearized relation for incident and reflected P-waves has been rewritten in 3 terms, related to their angle dependencies,

$$R_{PP}(\phi) = \frac{1}{2}\frac{\Delta Z}{Z} + \frac{1}{2}\frac{\Delta c_P}{c_P}\tan^2\phi - 2\gamma^2\frac{\Delta\mu}{\mu}\sin^2\phi \qquad (1)$$

with $\gamma = c_S/c_P$. Using this relation means that we estimate relative contrasts in acoustic impedance Z, P-wave velocity *cp* and shear modulus μ. The assumptions we make for the linearization of the full Zoeppritz equation are small angles of incidence (smaller than the critical angle), small relative contrasts and a single interface between two half spaces. The linear Zoeppritz model is given in the following matrix notation,

$$\vec{d} = \underline{\mathbf{A}}\vec{\lambda} + \vec{n}, \qquad (2)$$

where $\vec{d}$ represents the data vector, $\vec{\lambda}$ the elastic contrast parameter vector $(\frac{\Delta Z}{Z}, \frac{\Delta c_P}{c_P}, \frac{\Delta\mu}{\mu})^T$, $\underline{\mathbf{A}}$ the linearized Zoeppritz matrix and finally the vector $\vec{n}$ represents the nonlinear terms, the noise and the errors. As shown by others (for example Lörtzer and Berkhout [1993]) the acoustic impedance is much stronger present in the data than the angle-dependent parameters. Using empirical relations between the Z contrast and the cp and μ contrast respectivily, the inversion result can be constrained.

Apparent AVA due to different illumination angles and interference

The influence of the angle of illumination in a horizontally layered medium with constant velocity cp is shown in Figure 1. In Figure (A) a horizontal plane wave with a wavelength λ travels downward. Along the z-axis the wavelength λ_z equals λ, so in this example approximately 2 times the layerthickness. In Figure (B) a plane wave with a wavelength λ travels downward with an angle ϕ. Along the z-axis the wavelenght λ_z equals $\lambda/cos\phi$, so approximately 3 times the layerthickness in this example. This means that for higher angles a larger number of boundaries interfere than for smaller angles. This changing λ_z with offset in seismic data introduces an apparent AVA behavior. In order to remove this effect we should look with a constant band of λ_z for different offsets at the reflectivity. In this way we image an offset consistent reflectivity from our seismic data. This angle-dependent reflectivity imaging is further discussed in a companion paper [Wapenaar et al., 1995]. Note that the largest offset determines the resolution λ_z.

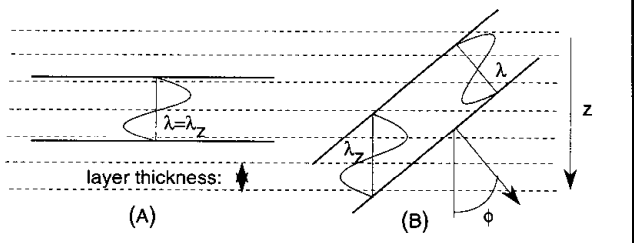

Figure 1: Horizontal layered medium showning angle-dependent spatial bandwidth λ_z.

Proposed inversion scheme using iterative angle-dependent reflectivity imaging

As shown in the previous section the inversion should be done on angle-dependent imaged reflectivity gathers. This means that for a large maximum angle we loose resolution in the near traces. In order to use the full amount of data we should start with a small band of λ_z but a large range of angles. We apply the elastic inversion on the imaged reflectivity gather (I) and save the estimated contrast parameters. Next we can use a larger range of λ_z but a smaller range of angles in the reflectivity imaging. We can again apply the elastic inversion process on this imaged reflectivity gather (II). We can use the results of the first inversion process (I) as 'a priori knowledge on a broader scale' in the second inversion process. We can continue this process in several steps until we have almost the whole range of λ_z and a small range of angles. Note that for subsequent iterations the a priori information contains more and more angle dependent information (from previous iterations), and the data less and less angle dependent information.

On the other hand the intercept or acoustic impedance is better determined by the data with a higher resolution. Using this scheme we use all the available data at 'different scales' in a correct way.

ZLF processing and determination of the ZLF-residue

In the constrained linear elastic inversion process the mismatch between the measured AVA and the Zoeppritz modeled AVA together with the mismatch between the a priori information and the estimated parameters is minimized. We can now use the final estimated contrast parameters for forward Zoeppritz modeling. This shows us the reflectivity as function of offset we have estimated. In other words we remove all nonlinear effects and the noise from our model, by applying a Zoeppritz-driven Linear Filtering (ZLF) process, given by

$$ZLF = \underset{\sim}{\mathbf{A}}\vec{\lambda} = \vec{d} - \vec{n}. \quad (3)$$

The difference between the measured reflectivity and the ZLF gather gives us the ZLF residue for all times and offsets,

$$residue = \vec{d} - \underset{\sim}{\mathbf{A}}\vec{\lambda} = \vec{n}. \quad (4)$$

This residue shows all the noise and all nonlinear events which are not incorporated in the linearized Zoeppritz model.

offset sections

Using the ZLF gathers and the ZLF residue we can now make common offset sections of the filtered data at any offset we choose. Also we can make residue sections at any offset we choose.

ZLF-residue analysis

In the following section we will discuss and show on the ZLF-residues and residue offset sections the influence of the factors mentioned in the introduction.

velocity or non-alignment errors

Several methods can be used to compute the AVA for a range of time or depth values. If the amplitudes are taken along a straight line from NM0 corrected CMP gathers or migrated gathers, all misalignments have a strong influence on the AVA curve. In Figure 2 a NM0 corrected CMP gather is shown with an error in the NM0 velocity and the AVA curves for the misaligned and correct aligned gathers around 1 .0s. The 4 percent error in the NM0 velocity gives a complete different AVA behavior, compared with the correct AVA curve shown by the stars.

multiples and conversions

Multiple reflections and converted reflections are not incorporated in our linear model. This means that they should show up in the ZLF-residue and not in the ZLF gather. In Figure 3 a real data example is given with a CMP gather after NM0 correction and after ZLF processsing. Also the ZLF-residue is shown. Clearly in the deeper part of the data and for larger offsets we see multiple and converted refections in the ZLF residue. The ZLF gather on the other hand shows clearly the linear part of the PP-reflections.

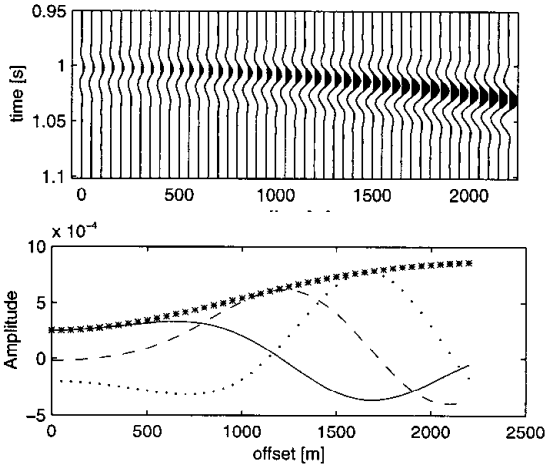

Figure 2: NM0 corrected CMP gather with 4 percent wrong NM0 velocity and AVA curves at 1.000s (solid), 1.008s (dashed), 1.016s (dots) and the correct AVA curve (no velocity error) at 1.000s (*).

angle dependent scales and interference

As shown in Figure 1, the illumination at offsets means illumination with an apparent longer wavelength (a larger λ_z). In the example with a single reflector in Figure 4A this shows up as stretching of the wavelet at larger offsets. This means that for a zero phase wavelet at the reflector, only the amplitude curve at the center peak of the wavelet versus the offset can be used for inversion. The AVA curves above and below the center peak are influenced by the stretching of the wavelet(Figure 4B). The data after applying the discussed reflectivity imaging, is shown in Figure 4C. Now for each offset the same range of λ_z has been used. If we take several AVA curves around the center peak, then they all show the same shape except for a wavelet dependent scalar (Figure 4D).

In a layered medium with an average layer thickness smaller than half the average λ_z the reflections will interfere. Due to different λ_z for different offsets, this interference will change with offset and therefore show an apparent AVA behavior, as shown in Wapenaar et al. [1995]. The same medium as used in this companion paper is used in our inversion scheme with and without angle-dependent reflectivity imaging. The data has been modeled using a real density log with contstant P-wave velocity and a zero S-wave velocity (acoustic medium). Hence the AVA curves should not be angle-dependent. It is obvious that the estimated contrasts in P-wave velocity and shear modulus without angle-dependent reflectivity imaging are erroneous. In this example we examine the ZLF residue offset sections for the elastic inversion with and without angle-dependent reflectivity imaging. The ZLF gather without angle-dependent imaging is shown in Figure 5A. The acoustic impedance is normally well estimated because it is strongly present as angle independent parameter in the measured data. One would therefore expect a small residue for small offsets.

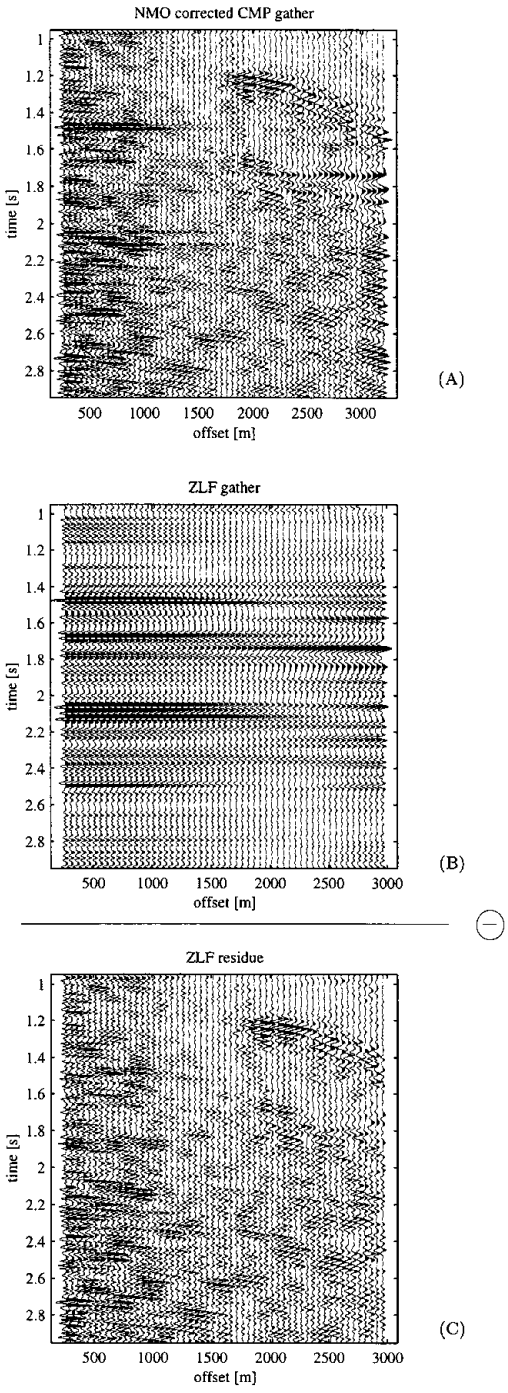

Figure 3: NM0 corrected CMP gather, ZLF processed gather a ZLF residue.

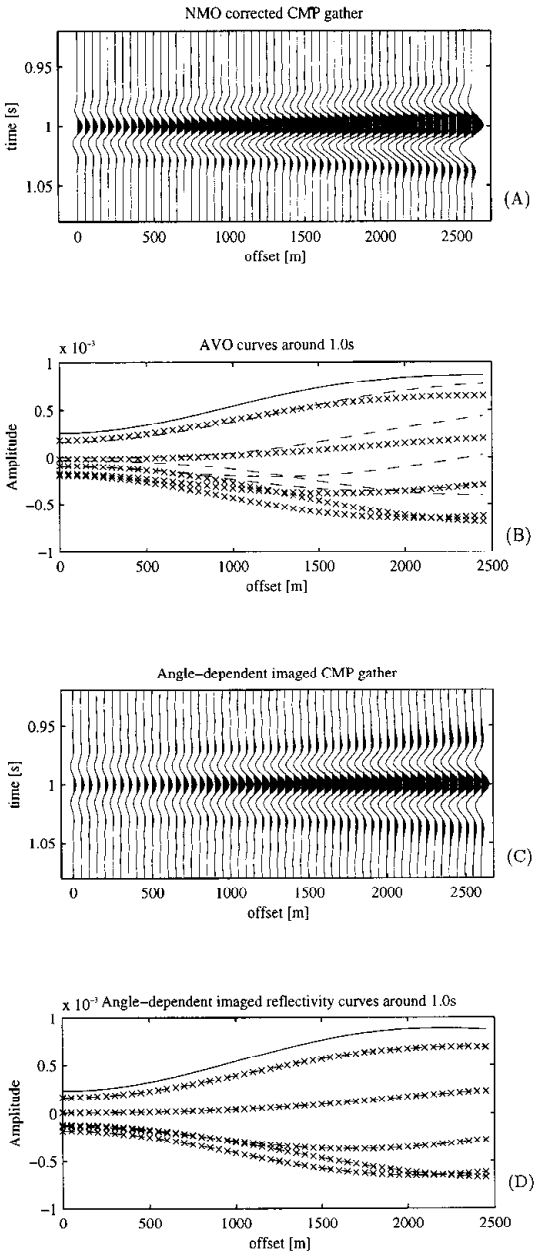

Figure 4: (A) NM0 corrected CMP , (B) AVA curves: 1000ms solid line, 980-996ms (step 4ms) cross lines, 1004-102Oms (step 4ms) dashed lines, (C) angle-dependent imaged CMP and (D) the same AVA curves with angle-dependent reflectivity imaging.

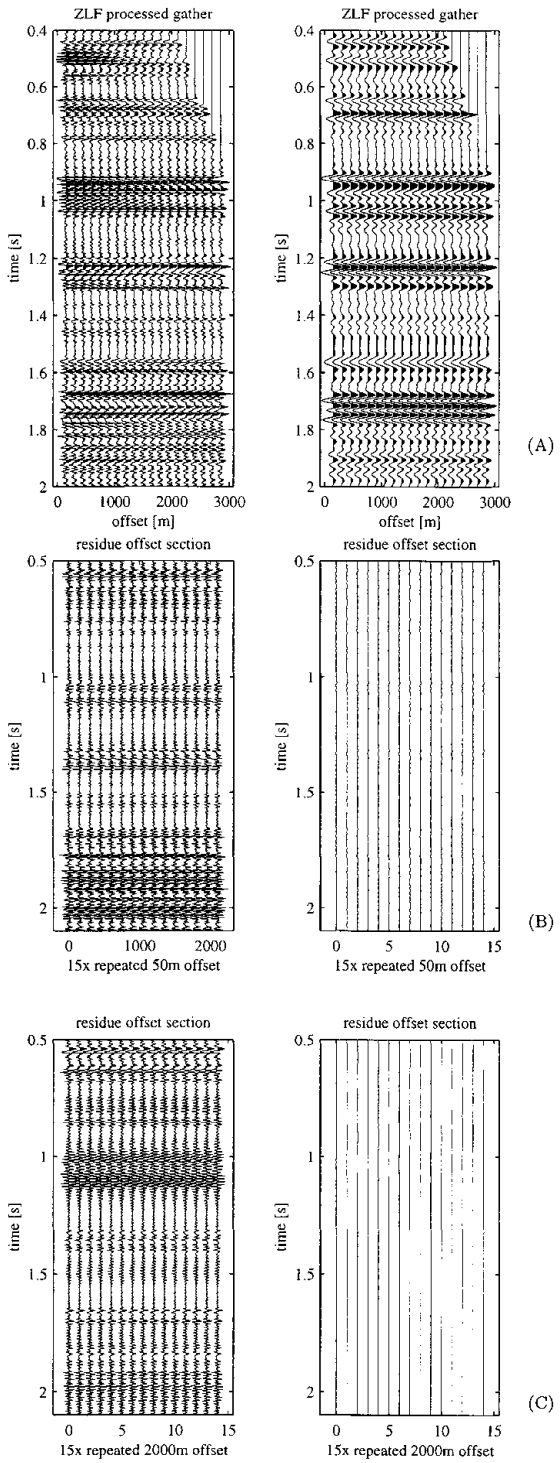

Figure 5: The results of the inversion without (left column) and with (right column) angle-dependent reflectivity imaging. (A) ZLF gathers, (B) residue offset sections at 50m and (C) residue offset sections at 2000m.

Nevertheless the ZLF residue at 50m offset without angle-dependent imaging, as shown in Figure 5B, shows a fairly large residue. This residue is of the same order as the residue at 2000m, as shown in Figure 5C. The ZLF residue at 50m offset of the angle-dependent imaged reflectivity, can be neglected. This is explained by the fact that the inversion is done for an 'averaged' λ_z. This 'averaged' λ_z is slightly larger than the λ_z at the near trace, resulting in a ZLF residue. After angle-dependent imaging there is no difference in λ_z with offset, resulting in a small residue. The density contrast can be computed by the difference of the estimated acoustic impedance and the P-wave velocity contrast. In Figure 6 the integral over the estimated density contrast and the actual contrast are displayed, showing an excellent match.

Conclusions

In this paper we have presented the ZLF process and the ZLF residue as a convenient way of presenting the results of constrained linearized elastic inversion. The estimated linear AVA behavior is shown in the ZLF gather and the nonlinear terms and noise are shown for all times and offsets in the ZLF-residue. Using offset sections the behavior can be examined along a line for each desired offset.

In the residue analysis we have shown that the errors due to misalignment and due to comparing different scales or λ_z ranges have a major influence on the accuracy of the inversion results. An angle-dependent reflectivity imaging should be applied before any Zoeppritz-like inversion process can be applied. By using a iterative inversion scheme all data can be used without loosing resolution.

References

Aki, K., and Richards, P. G., 1980, Quantitative seismology: Theory and methods: W.H.Freeman and Co.

Lörtzer, G. J. M., and Berkhout, A. J., 1993, Linearized AVO inversion of multicomponent seismic data *in* Castagna, J. P., and Backus, M. M., Eds., Offset-dependent reflectivity - Theory and practice of AVO analysis:: Soc. Expl. Geophys., 317-332.

Wapenaar, C. P. A., van der Leij, T. S., and van Wijngaarden, A. J., 1995, Ava and the effects of interference: 65th annual SEG meeting, Houston, SEG, Expanded Abstracts.

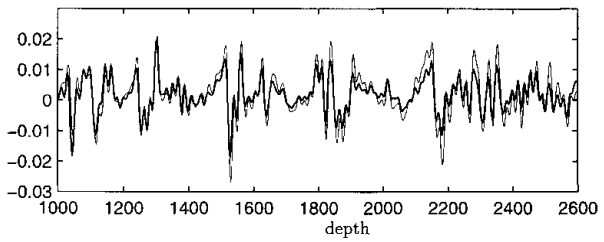

Figure 6: The integral over the estimated density contrast (thick line) and over the actual (well) density contrast (thin line).